Supporting Information for

Towards room-temperature stable topological magnetic semiconductors based on two-dimensional Janus vanadium chalcogenides

Shuo Zhang,[1] *Yunfei Zhang,*[1] *Minghao Jia,*[2] *Dan Xing,*[2] *Lixiu Guan,*[2,*] *and Junguang Tao*[1,3,*]

[1]*School of Materials Science and Engineering, Hebei University of Technology, Tianjin 300132, China*

[2]*School of Science, Hebei University of Technology, Tianjin 300401, China*

[3]*Hebei Engineering Laboratory of Photoelectronic Functional Crystals, Hebei University of Technology, Tianjin 300132, China*

*Emails of the corresponding authors: lixiuguan@hebut.edu.cn (L.G.); jgtao@hebut.edu.cn (J.T.)

Contents

Section 1. Electronic structure and stability

Section 2. Magnetic configurations of ML VXY

Section 3. Influence of E-field on charge redistribution, band structure and exchange interaction for VXY

Section 4. Effect of temperature and B-field on topological spin textures

Section 5. Dynamics of labyrinth-skyrmion mixed (LSM) domain with respect to B-field

Section 6. Skyrmion transistor designed based on VSSe

Section 1. Electronic structure and stability

For monolayer (ML) Janus VSTe and VSeTe, the CBM and VBM are located at K and Γ points, respectively. The CBM is mainly contributed by V d_{z^2} orbital. However, the contribution to VBM is different: in VSTe, it is mainly from V d_{z^2} orbital, while in VSeTe, it is primarily from V d_{xz} and d_{yz} orbitals.

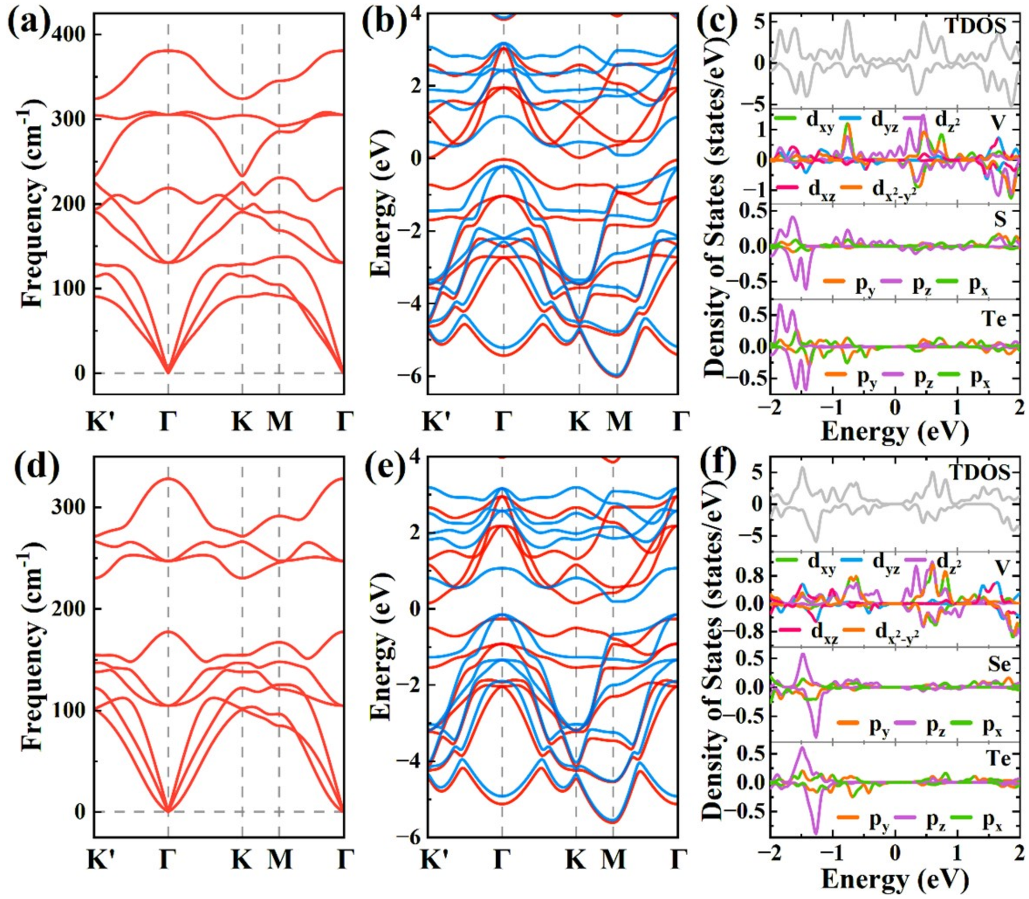

Figure S1. (a, d) Phonon dispersion spectra, (b, e) spin-polarized electronic band structures, and (c, f) the corresponding total density of states (TDOS) and projected density of states (PDOS) of ML Janus VSTe and VSeTe.

To affirm the stability of ML Janus VXY system, we performed phonon dispersion calculations, the results are depicted in Fig. 1(b) and Figs. S1(a, d). There are no imaginary frequencies for all phonon dispersion curves, which substantiates the dynamic stability of the materials. Furthermore, to examine its thermal stability, ab initio molecular dynamics (AIMD) simulations were executed, as illustrated in Fig. S2. Upon subjecting the system to a temperature of 300 K over a period of 8 ps, no structural reconstruction or bond dissociation was detected. This observation corroborates the thermodynamic stability of ML Janus VXY, indicating that it maintains its integrity and does not undergo any significant morphological changes even at elevated temperatures.

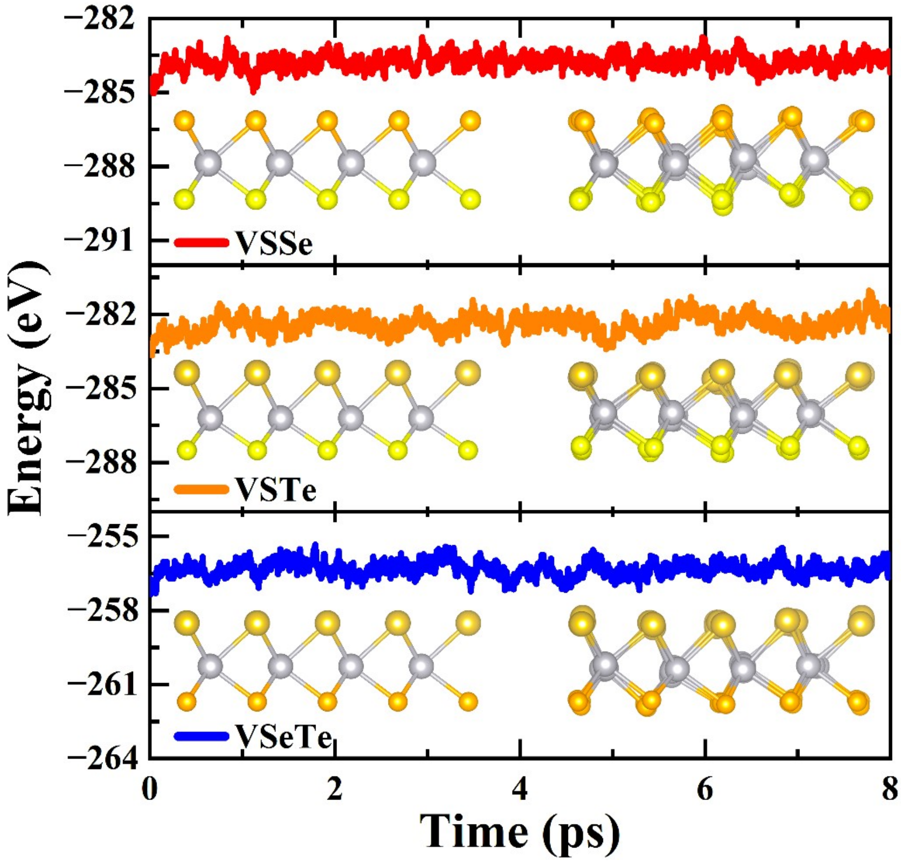

Figure S2. Total energy evolutions of ML Janus VXY within 8 ps at 300 K according to AIMD simulations.

Section 2. Magnetic configurations of ML VXY

To determine the spin ground state of ML VXY, two spin configurations were considered for each system, as shown in Fig. S3. Table S1 summarizes the energies of ferromagnetic (FM) and stripy antiferromagnetic (AFM) magnetic configurations in VSSe, VSTe, and VSeTe systems. The results indicate that FM configuration has the lowest energy for all systems, making it the most stable magnetic configuration.

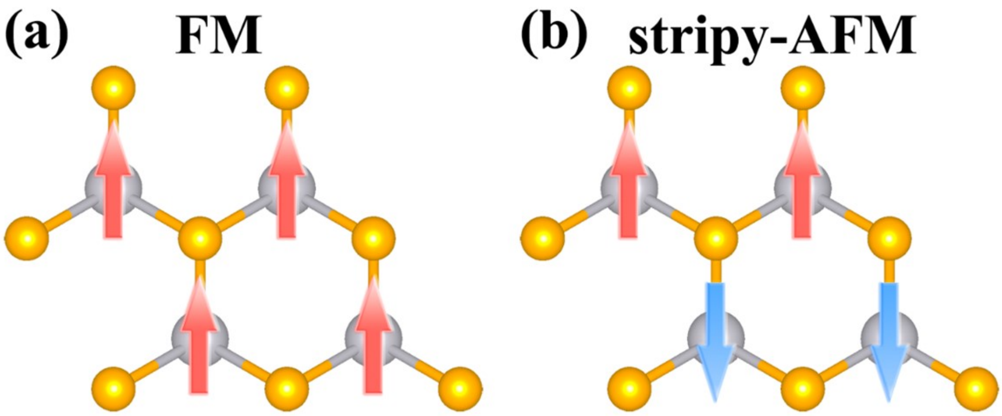

Figure S3. Schematic diagram of FM and stripy-AFM spin configurations for ML VXY.

Table S1. Relative energies of VSSe, VSTe and VSeTe systems in different magnetic states with respect to FM states, ($E-E_{FM}$)

.	E_{FM} (meV/unit cell)	$E_{stripy-AFM}$ (meV/unit cell)
VSSe	0.0	100.5
VSTe	0.0	71.2
VSeTe	0.0	107.1

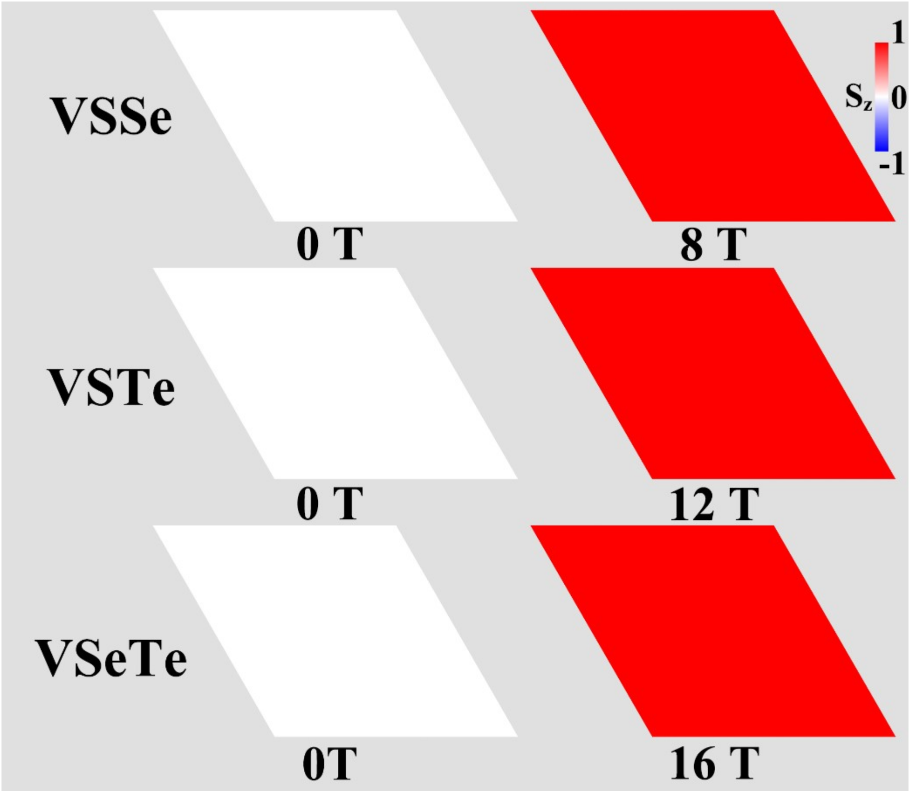

Figure S4. Spin orientations of VSSe, VSTe, and VSeTe without an electric field, with and without the influence of a magnetic field.

Section 3. Influence of E-field on charge redistribution, band structure and exchange interaction for VXY

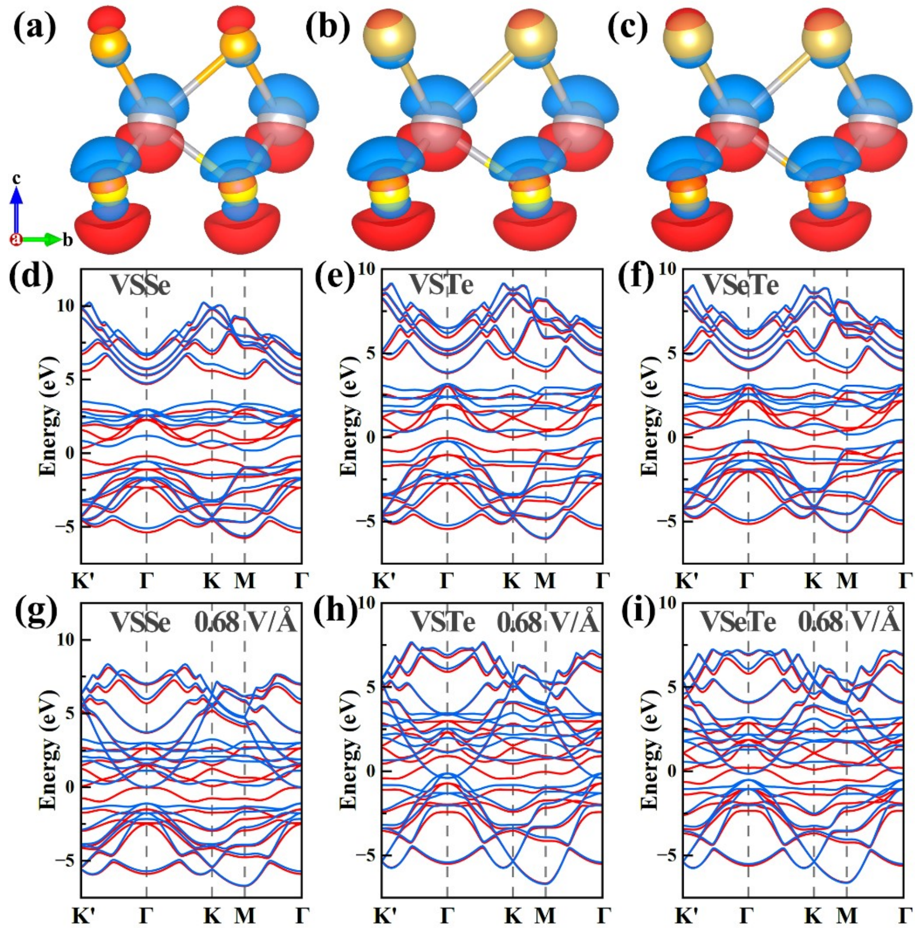

Figure S5. Differential charge density contours for VSSe (a), VSTe (b), and VSeTe (c), showcasing the impact of E-field in comparison to that without E-field. The blue and red contours represent electron depletion and accumulation regions, respectively. The isosurface value is 1×10^{-5} e/Å^3. The band structures of VSSe, VSTe, and VSeTe without (d-f) and with 0.68 V/Å E-field (g-i), respectively.

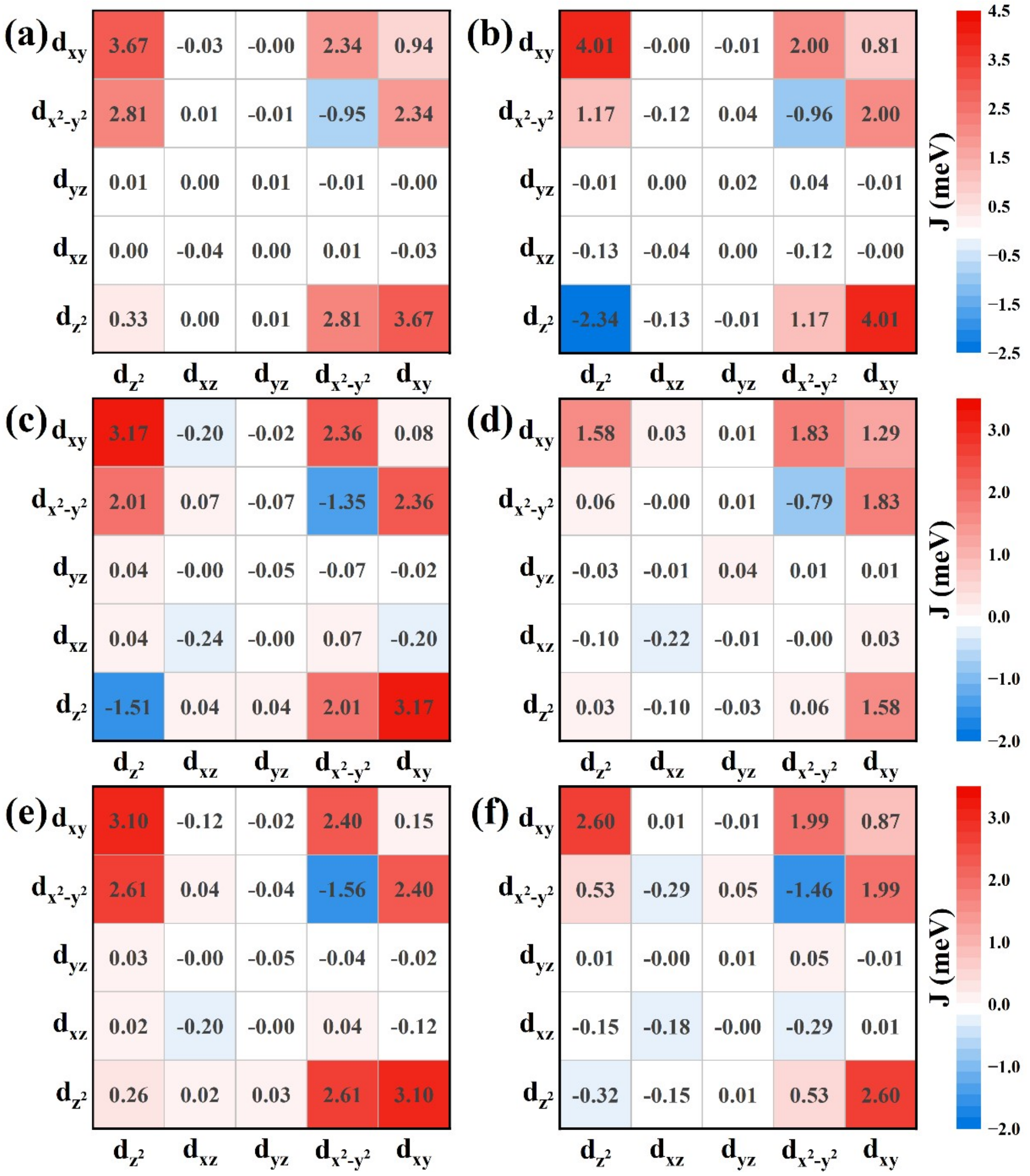

Figure S6. Changes in exchange coefficients of V *d* orbitals in VSSe (a, b), VSTe (c, d), and VSeTe (e, f). The left-side panels show the situation without E-field, while the right-side ones are with an E-field of 0.68 V/Å.

Section 4. Effect of temperature and B-field on topological spin textures

As illustrated by the micromagnetic simulations, the VSTe system exhibits changes of skyrmion sizes, ranging from a maximum diameter of 15.23 nm to a minimum of 10.87 nm. Similarly, the VSeTe system presents skyrmions with diameters that vary from 7.72 nm down to 6.41 nm. When the perpendicular magnetic field (B-field) is inverted, which entails a transition of magnetization from a positive to a negative state, the topological charge of the skyrmions undergoes a corresponding reversal in sign as well. This phenomenon highlights the pivotal role of the B-field in modulating the characteristics and stability of skyrmions, which is a critical consideration in the development of skyrmion-based technologies.

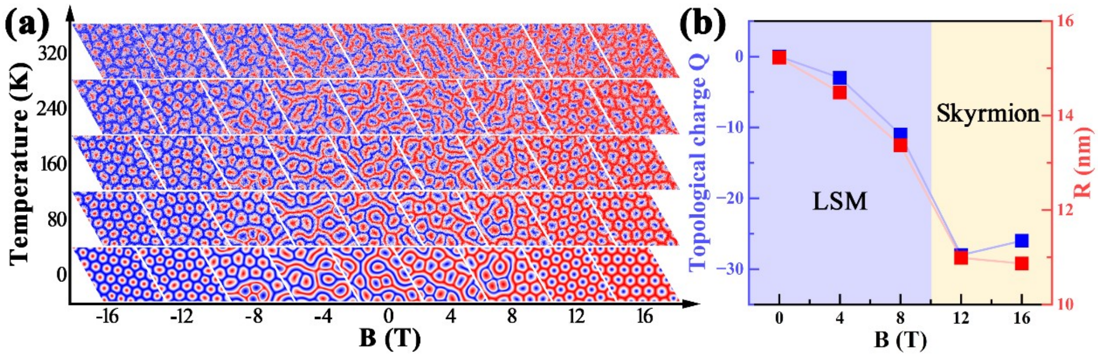

Figure S7. Spin textures and topological properties of ML Janus VSTe under different B-field and temperature. (a) Spin texture as a function of temperature under different B-field. (b) The relationship between topological charge and skyrmion radius with respect to B-field at 0 K.

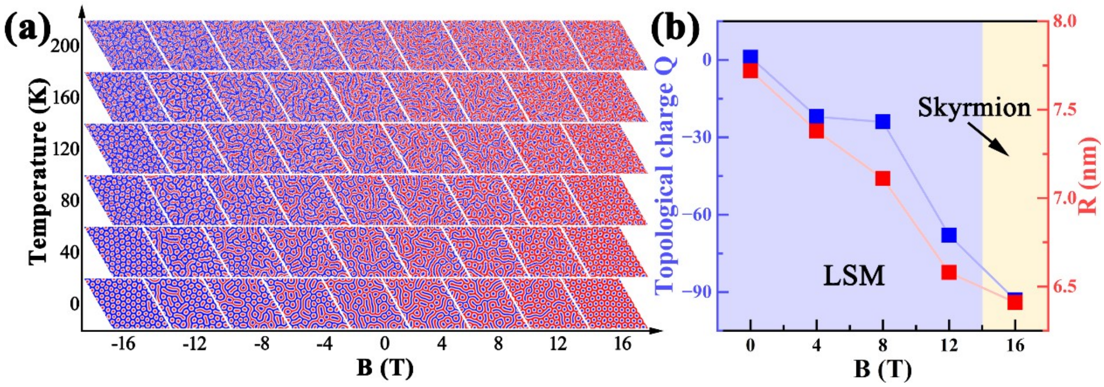

Figure S8. Spin textures and topological properties of ML Janus VSeTe under different B-field and temperature. (a) Spin texture as a function of temperature under different B-field. (b) The relationship between topological charge and skyrmion radius with respect to B-field at 0 K.

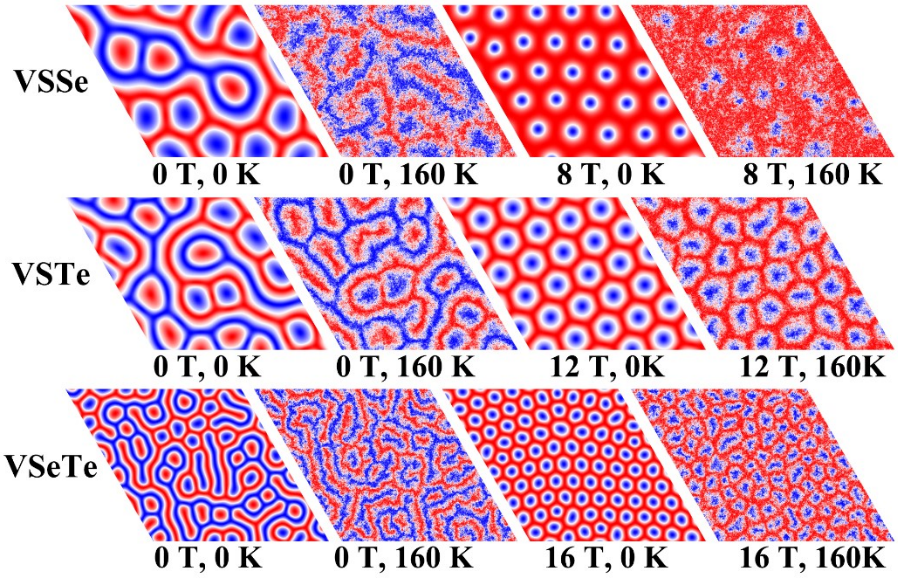

Figure S9. Influence of B-fields and temperature on skyrmions in VSSe, VSTe, and VSeTe.

The evolution of spin textures in VSSe, VSTe, and VSeTe systems under varying temperature and B-fields is depicted in Fig. S9. Under the conditions of 0 T and 0 K, VSSe, VSTe, and VSeTe are all characterized by wormlike magnetic domains and dispersed skyrmions, exhibiting the LSM phase. Upon elevating the temperature to 160 K, a phase transition is observed across all systems, shifting towards the wormlike phase. This transition is occurred by the fact that, at 0 K, the intrinsic skyrmions are separated from domains by a very short distance. As the temperature rises, these skyrmions progressively merge with the domains. Under the conditions of 8 T and 0 K for VSSe, 12 T and 0 K for VSTe, and 16 T and

0 K for VSeTe, all systems adeptly form the skyrmion phase, wherein the skyrmions exhibit a concentric circular arrangement. As the temperature increases to 160 K, the skyrmions undergo some deformation but retain their topological magnetic properties, highlighting the robustness of the skyrmion phase.

Section 5. Dynamics of labyrinth-skyrmion mixed (LSM) domain with respect to B-field

The LSM phase is a combination of wormlike domains and skyrmions. In an effort to explore the interrelation between the domain of the wormlike phase and the external B-field, we conducted an examination of the spin structures across the VXY systems within a B-field range spanning from 0 to 8 T. Figure S10 and Fig. 4 show that at 0 T, all systems are characterized by the LSM phase. Owing to differences in the magnetic parameters of VSSe, VSTe and VSeTe, there are observable variations in skyrmion size, domain width, and the density of the wormlike phase. Notably, the VSSe system exhibits the largest skyrmion size, the most expansive domain, and the lowest wormlike phase density, whereas the VSeTe system manifests the converse attributes. The principal driver of these discrepancies is attributed to the variation in the ratio of the Dzyaloshinskii-Moriya interaction (DMI) to the exchange constant ($|\boldsymbol{d}_{||}|/J$ ratio).

To systematically investigate the relationship between domain and the external B-field, we analyzed four parameters: domain average width

(W_{avg}), effective length (L_{eff}), L_{eff}/W_{avg} ratio, and the proportion of domain area (A_{dom}). Given the consistent W_{avg} of the domain despite their varied shapes, we determined their L_{eff} by dividing the domain area by its W_{avg}. Figure S11 shows the correlation between these domain parameters and the B-field for VSTe and VSeTe systems. In the case of VSTe [Figs. S11(a, b)], at 0 T, the LSM phase predominantly exhibits a wormlike domain structure, while between 4 and 8 T, it is primarily composed of numerous skyrmions and reduced wormlike domains. Additionally, Figure S11(b) shows that the proportion of A_{dom} decreases from 35.95% to 16.27%, which is attributed to a significant phase transition within the LSM phase. For VSeTe [Figs. S11(c, d)], as the B-field intensifies, there is a gradual reduction in the domain's W_{avg}, L_{eff}, L_{eff}/W_{avg} ratio, and A_{dom} proportion, without any abrupt phase transitions. For VSSe, at 0 T, the values of W_{avg}, L_{eff}, L_{eff}/W_{avg} ratio, and A_{dom} proportion are 24.5 nm, 757.66 nm, 30.93, and 29.08%, respectively. In essence, compared to VSTe and VSeTe, the spin textures generated in VSSe exhibit a heightened sensitivity to B-field. Furthermore, the L_{eff}/W_{avg} ratios of VSSe and VSTe are significantly lower than that of VSeTe by an order of magnitude, indicating that these two materials are more conducive to the design of skyrmion-based devices. In short, VSSe, with its adjustable phase structure and smaller skyrmion size, presents an exemplary platform for the conceptualization of nanoscale spintronic devices, offering a high degree of tunability and control over magnetic properties.

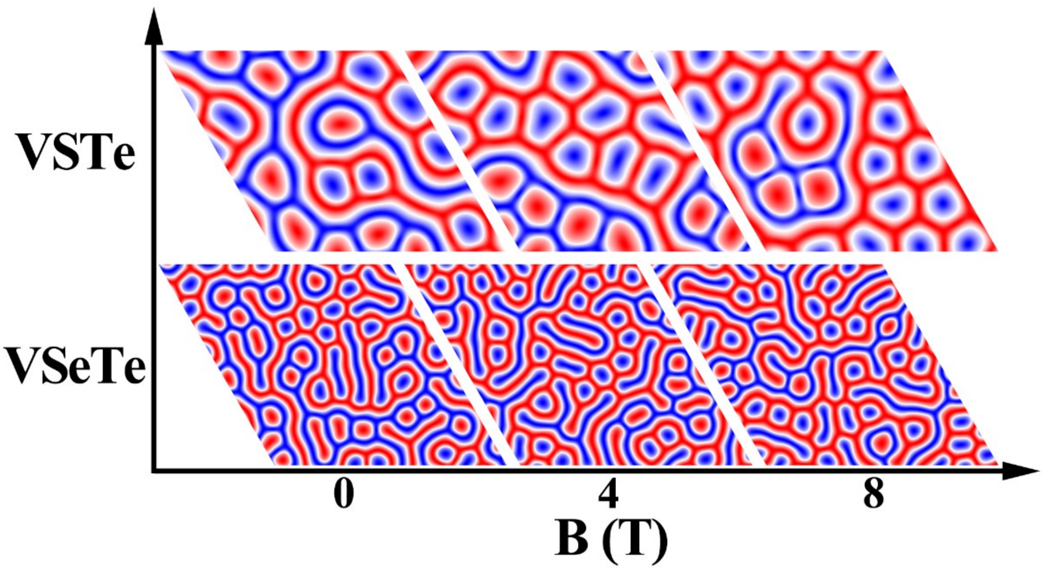

Figure S10. Spin textures generated in VSTe and VSeTe systems under different B-field.

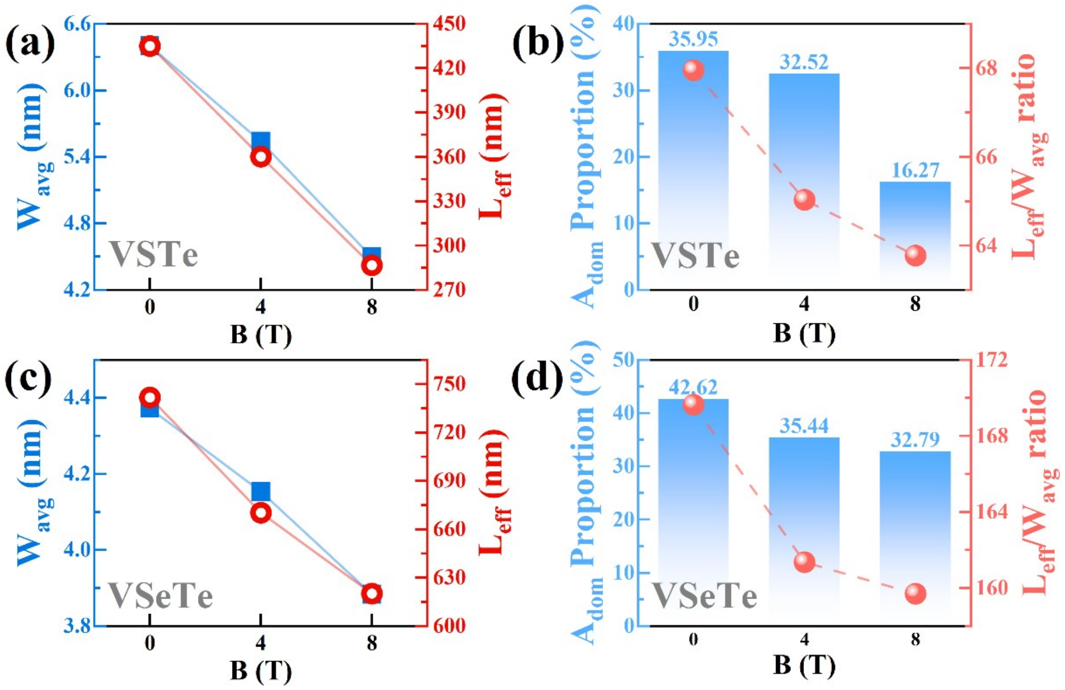

Figure S11. Domain variations in VSTe and VSeTe systems as a function of B-field. (a, c) Changes in domain average width (W_{avg}) and effective length (L_{eff}) with different B-fields. (b, d) Changes in the L_{eff}/W_{avg} ratio and domain area (A_{dom}) proportion with B-field.

Section 6. Skyrmion transistor designed based on VSSe

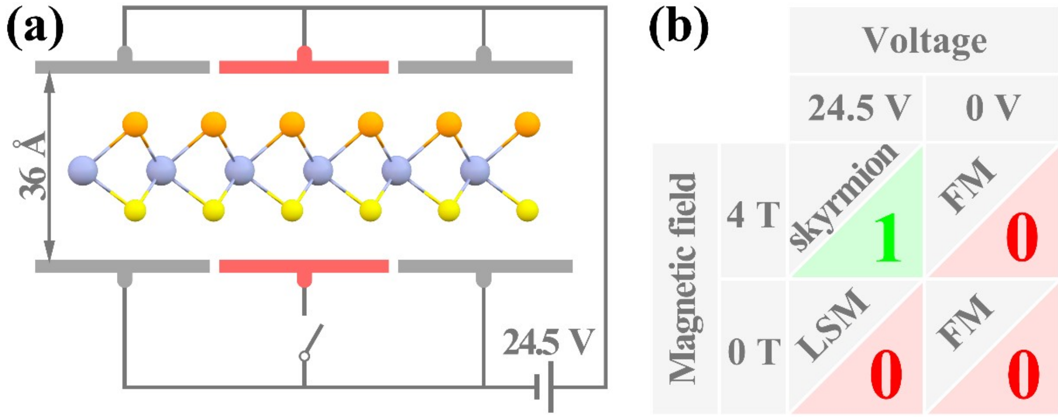

Figure S12. (a) The circuit diagram of the skyrmion transistor, with the red region corresponding to E-field-controlled region. (b) The phases generated in E-field-controlled region under different B-field and voltage conditions, along with the corresponding transistor states. Here, 1 (green) represents the "ON" state, and 0 (red) represents the "OFF" state.